

Linear Optical and Third-Order Nonlinear Optical Properties of Some Fluorenyl- and Triarylamino-Containing Tetracyanobutadiene Derivatives

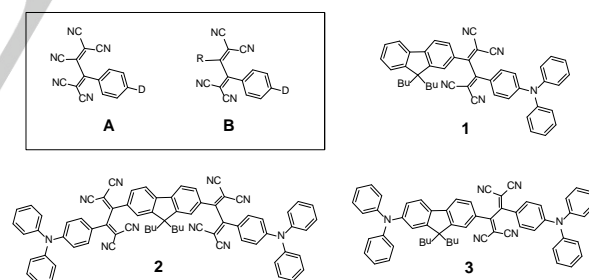
Ziemowit Pokladek,^[a] Nicolas Ripoche,^[b,c] Marie Betou,^[d] Yann Trolez,^{*,[d]} Olivier Mongin,^[b] Joanna Olesiak-Banska,^[a] Katarzyna Matczyszyn,^{*,[a]} Marek Samoc,^[a] Mark G. Humphrey,^[c] Mireille Blanchard-Desce^[e] and Frédéric Paul^{*,[b]}

Abstract: We report the synthesis and characterization of four new tetracyanobutadiene (TCBD) derivatives (**1-3** and **2'**) incorporating 2- or 2,7-fluorenyl and diphenylamino moieties. The electroactivity of **1-3** and **2'** was studied by cyclic voltammetry (CV), while the linear optical and (third-order) nonlinear optical (NLO) properties were investigated by electronic spectroscopy and Z-scan studies, respectively. All experimental investigations were rationalized by DFT computations, providing an insight into the electronic structure of these derivatives and on their application potential. We show that these derivatives are non-luminescent in solution at ambient temperatures, but become fluorescent in solvent glasses. This finding constitutes an unprecedented observation for TCBD derivatives. Also, we show by Z-scan studies that these derivatives behave as two-photon absorbers in the near-IR range (800-1050 nm). These third-order NLO properties are discussed and compared with those of their alkynyl precursors (**4-6**), which have been investigated by two-photon excited fluorescence (TPEF).

Introduction

Tetracyanobutadienes (TCBDs) and, more generally, polycyanoethylenes are powerful acceptor groups,^[1] which,

when conjugated to donor groups through an unsaturated spacer such as in **A** (Scheme 1), have been demonstrated to give rise to donor-acceptor molecular structures possessing remarkable non-resonant quadratic^{[1], [2]} and cubic^[3] nonlinear optical (NLO) responses.^[4] Furthermore, in the latter case, the seminal investigations of the Diederich group have clearly shown that related derivatives such as **B** (R = C≡C(4-C₆H₄NMe₂); D = NMe₂) hold outstanding promise in the field of integrated nonlinear optics, given that these structures possess a large off-resonant cubic nonlinear molecular polarizability (γ_0) and give rise to high quality films by molecular beam deposition on glass supports.^[5] These remarkable features can be attributed to the non-planar tetracyanobutadiene (TCBD) core which, while being thermally very stable and strongly electron-withdrawing, adopts a non-planar conformation. It therefore limits any unwanted crystallization during the thermal deposition process, a very desirable property for the realization of optical devices such as waveguides.^[6]



Scheme 1. Molecules targeted in this work and selected polycyanoethylene derivatives (see inset).

However, apart from these promising results obtained with a handful of molecules, much remains to be learned about the third-order nonlinear optical properties of cyanoethylene derivatives, in particular regarding their two-photon absorption (2PA) capabilities.^[4] To the best of our knowledge, this particular cubic NLO property which is related to the imaginary part of γ has only been briefly examined,^[7] and never with TCBD derivatives. Increasing our knowledge of 2PA cross-sections at specific wavelengths would strengthen interest in such molecules for integrated nonlinear optics, by opening the possibility to use them in multi-photon optical gates^[8] or in related devices for optical limiting or pulse shaping.^[7b] More

[a] Z. Pokladek, Dr J. Olesiak-Banska, Dr. K. Matczyszyn, Pr. M. Samoc

Advanced Materials Engineering and Modeling Group
Faculty of Chemistry
Wroclaw University of Technology
50-370 Wroclaw

[b] N. Ripoche, Dr. O. Mongin, Dr. F. Paul
Institut des Sciences Chimiques de Rennes, CNRS (UMR 6226)
Université de Rennes 1
Campus de Beaulieu, 35042 Rennes Cedex (France)
Tel: (+33) 02-23-23-59-62
E-mail: frederic.paul@univ-rennes1.fr

[c] Pr. M. G. Humphrey
Research School of Chemistry, Australian National University
Canberra, ACT 2601 (Australia)

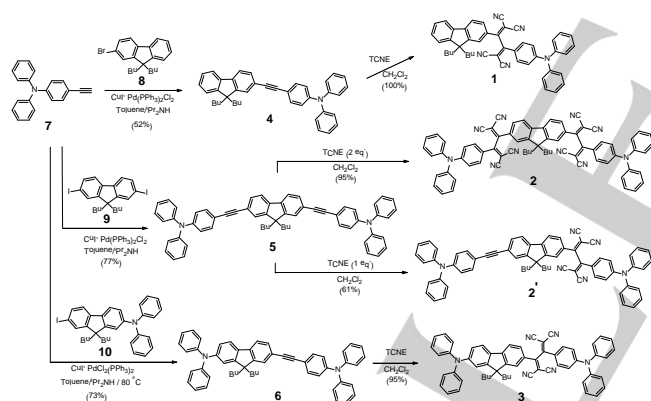
[d] Dr. M. Betou, Dr. Y. Trolez
Ecole Nationale Supérieure de Chimie de Rennes,
Institut des Sciences Chimiques de Rennes, CNRS (UMR 6226)
11 allée de Beaulieu, CS 50837
35708 Rennes Cedex 7 (France)

[e] Dr. M. Blanchard-Desce
ISM, CNRS (UMR 5255)
Université Bordeaux
33400 Talence France

generally, the lack of information about the 2PA capability of such stable, conjugated and strongly polarized species is also unfortunate because multi-photon absorbers are key to many other important societal applications,^[9] such as optical information storage, nanofabrication, photodynamic therapy, and, when fluorescent, molecular imaging.^[7b]

With this in mind, an investigation into the 2PA properties of a series of TCBD derivatives (**1-3** in Scheme 1) incorporating fluorenyl and diphenylamino moieties was initiated, because these two building blocks are often constituents of good two-photon absorbers.^[10] In addition, we were also wondering if the strongly fluorescent fluorenyl unit^[11] could have any positive effect on the luminescence of the targeted compounds.^[10f, 12] Indeed, luminescence is a highly desirable feature for two-photon absorbers in biomedical applications.^[7b, 9a] However, the scant data available in the literature about the luminescence of TCBD derivatives suggest that such species will in general be poor luminophores.^[13] We thus report hereafter the synthesis of **1-3** and the study of their linear optical and cubic nonlinear optical properties, with a particular emphasis on their 2PA capabilities. Comparison between **1** and **2** should evidence the influence of the (dipolar vs. symmetric and multipolar) molecular structure on these properties, while comparison between **1** and **3** should reveal the influence of a donor group appended to the 2- or 2,7-fluorenyl fragment.

Results and Discussion



Scheme 2. Synthesis of **1-3** and **2'**.

Synthesis of the compounds. The target compounds **1-3** were obtained from the corresponding alkyne derivatives **4-6** in one step by tetracyanoethylene (TCNE) cycloaddition at room temperature (Scheme 2).^[4] Following reaction of one equivalent of TCNE with **5**, the mono-addition adduct **2'** could also be cleanly isolated in 61% yield, while the double-addition adduct **2** was isolated in 19% yield in the same experiment. The required precursor alkynes **4-6** were themselves obtained by Sonogashira couplings from the known starting compounds **7**,^[14] **9**^[15] and **10**.^[10c] The latter precursor was synthesized from **9** and diphenylamine, in a similar fashion to the synthesis of its dodecyl analogue.^[16] All the new compounds **1-6** and **10** were fully characterized and their structures were unambiguously established by mass spectrometry and by the combined use of

NMR (for **1-3**, a combination of COSY and NOESY was used to assign all the observed protons) and IR/Raman spectroscopies, the latter techniques evincing the characteristic $\nu_{C=C}$ modes expected for these molecules (Experimental Section and ESI).

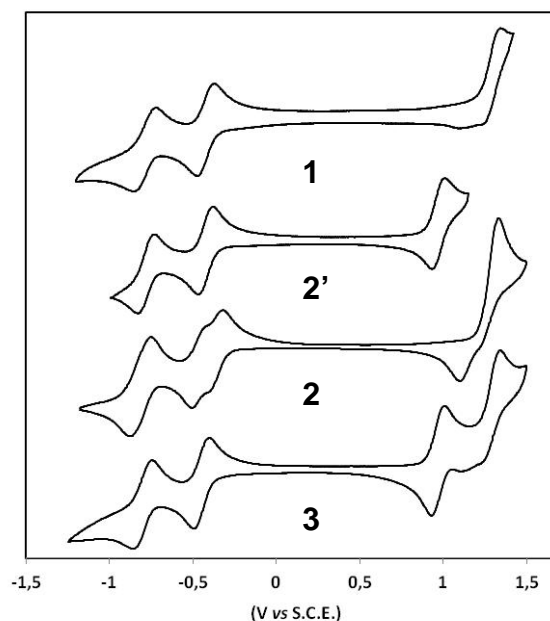


Figure 1. Cyclic voltammograms of **1-3** and **2'** in $\text{CH}_2\text{Cl}_2/[n\text{-Bu}_4\text{N}][\text{PF}_6]$ (0.1 M) at 25 °C at 0.1 V/s.

Cyclic Voltammetry. The electrochemical properties of **1-3** (Table 1) were then investigated by cyclic voltammetry (CV) in dichloromethane (Figure 1). As expected from previous studies and also from DFT calculations (see later),^[1b, 1c, 4] all these new derivatives are electroactive, the tetracyanoethylene moiety giving rise to two one-electron reductions located at each of the dicyanoethene moieties.^[3c] Thus, **1**, **2'** and **3** show a chemically-reversible reduction process at ca. -0.4 V followed by a second one near -0.7 V vs. SCE. The first reduction signal (around -0.4 V vs. SCE) of the derivative **2**, featuring two TCBD units, is split into two distinct waves which are separated by ca. 77 mV, revealing the existence of electronic communication between the two TCBD units symmetrically disposed at either side of the 2,7-fluorenyl linker. Interestingly, this splitting is not observed for the second reduction process of these TCBD units. The latter takes place at the potential observed for **2'**, indicating that the two additional electrons injected into the LUMO of this compound do not interact, or at least not to the same extent as those associated with the first reduction process. In accordance with DFT calculations, this indicates that the $\text{C}=\text{C}(\text{CN})_2$ subunits reduced first in **2** are most likely those located closer to the bridging ligand which may interact through its unsaturated π manifold, whereas the more remote 1,1-dicyanoethenyl units, closer to the electron-donating diphenylamino groups, are reduced in a subsequent and separate step at ca. 0.3 V more negative potentials. Based on the coincidence between the potential of the second reduction of **2** and those of **1**, **2'** and **3**, a similar behavior certainly takes place with the other TCBD derivatives. The compounds **1-3** and **2'** give also rise to electrochemical events at higher potentials, closer to 1.0 V vs. SCE. As suggested by the CVs of their precursor complexes (**4-**

6) and DFT calculations, these pseudo-reversible events (in the chemical sense) are not related to the presence of the TCBD units, but rather they correspond to the oxidation of the triaryl amino endgroups. Indeed, such a process is known to occur around 0.9 V vs. SCE,^[17] as observed in the present case for **4-6**. In **1-3** and **2'**, these oxidations are shifted to more positive values (by ca. 0.3 V) because of the presence of the nearby TCBD electron-accepting groups, rendering this oxidation thermodynamically less favored. The first of these waves, observed at lowest potentials in **2'** and **3**, likely corresponds to the oxidation of the diphenylamino group most remote from the TCBD group, while the second wave, at higher potentials (around 1.3 V vs. SCE), corresponds to the oxidation of the diphenylamino group closer to the TCBD group. Besides being indicated by DFT calculations, this ordering is also supported by the good match between the potential of the second oxidation process in **2'** and that observed for **1**. Both processes are chemically not reversible at a scan rate of 0.1 V/s. For the symmetric derivative **2** and also for its symmetric precursor **5**, the oxidation of the two diphenylamino substituents takes place in an apparent two-electron process, in line with a weak or non-existent electronic coupling between these moieties across the central spacer. Based on the Rehm-Weller equation (eq. 1),^[18] these data can be used to derive an estimate of the free enthalpy of formation of the intramolecular CT state at lowest energy (ΔG_{CT}). The latter is given by the difference between the first amino-based oxidation potential and the first TCBD-based reduction potential in a given solvent (Table 1), corrected by an electrostatic term. Presently, estimates of the distances „a“ in eq. 1 for **1-3** and **2'** could be obtained from molecular modelling studies (DFT) and the corresponding ΔG_{CT} values were computed (Table 2).^[19]

$$\Delta G_{CT} = E^{\circ}(D^{+}/D) - E^{\circ}(A/A^{\cdot-}) - e^2/4\pi\epsilon_0\epsilon a \quad (1)$$

Table 1. Electrochemical Data for **1-6**.^[a]

Cmpd/ E° [ΔE_p] ^[b]	2 nd reduction of TCBD	1 st reduction of TCBD	1 st oxidation of ArNPh ₂	2 nd oxidation of ArNPh ₂
1	-0.77 [1.1]	-0.41 [0.9]	1.31 [0.8] ^[c]	/
2'	-0.76 [1.1]	-0.40 [0.9]	1.00 [0.7]	1.31 [1.0] ^[c]
2	-0.79 [1.1]	-0.42 [0.9] -0.35 [0.9]	1.30 [0.9] ^[c]	/
3	-0.79 [1.3]	-0.42 [0.9]	0.99 [0.7]	1.31 [0.9] ^[c]
4	/	/	/	0.96 [0.8]
5	/	/	/	0.98 [0.7]
6	/	/	0.84 [0.6]	0.98 [0.7]

[a] Conditions: CH₂Cl₂ solvent, 0.1 M [^tBu₄N][PF₆], 20 °C, Pt electrode, sweep rate 0.100 V s⁻¹. [b] ΔE_p is the peak-to-peak separation; E° and ΔE_p values in V (\pm 5 mV) vs. SCE. [c] Chemically not reversible.

UV-Visible Absorption. The derivatives **1-3** and **2'** each exhibit a strong absorption extending beyond 700 nm in the visible range (Figure 2a) and giving them a dark-orange color.

According to DFT calculations (see later), these absorption bands correspond to several overlapped charge-transfer (CT) transitions from the electron-rich diphenylamino substituent(s) toward the electron-withdrawing TCBD/fluorenyl fragments (Table 2). Thus, the transitions at lowest energy correspond to CT transition(s) from the occupied MOs located on the diphenylamino groups toward the TCBD π^* MOs. Their large π - π^* character is supported by their overall weak (and somewhat erratic) solvatochromism (see ESI). Notably, their energy is always superior to the enthalpy of formation of the CT state (ΔG_{CT}) as derived by eq. 1. The next lowest-energy band(s) correspond to CT transition(s) toward the empty MOs on the fluorenyl/TCBD fragment. Finally, at higher energies, $\pi^* \leftarrow \pi$ CT transitions toward the TCBDs but originating from the fluorenyl fragments are observed. This holds for both the dipolar and multipolar derivatives **1** and **2**, except that in the latter case, the donor groups are twice as numerous, resulting in a rough doubling in intensity of the low-energy transitions. The increased absorption at lowest energy for the dipolar compounds **3** and **2'** and the stronger absorption near 350 nm in the latter compound can be explained by the presence of CT transitions taking place between the second diphenylamino group and the π^* MOs of the TCBD or fluorenyl fragments. Higher-energy transitions (around 300 nm and shorter wavelengths) involve additional CT transitions from the second diphenylamino group and π^* MOs of the fluorenyl, as well as $\pi^* \leftarrow \pi$ transitions more localized on the triphenylamino fragments.

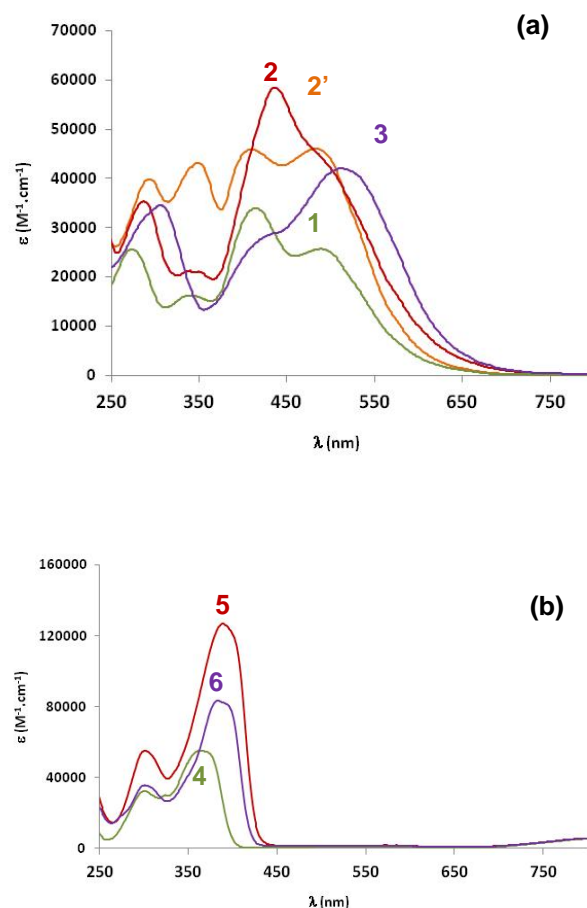


Figure 2. UV-Vis spectra of **1-3** (a) and **4-6** (b) in CH₂Cl₂ at 25 °C.

In comparison, their precursors **4-6** are much more transparent in the visible range (Figure 2b). Again, according to the DFT calculations (see ESI), their yellowish color originates from two transitions with significant $\pi-\pi^*$ character corresponding to a CT transition from the diphenylamino endgroup toward the fluorenyl group. The transition at lowest energy corresponds to the HOMO-LUMO transition; its large $\pi-\pi^*$ character is supported by the very weak solvatochromism exhibited by this band for **4-6** (see ESI). The dipole change associated with this transition is obviously rather weak.

Emission Studies. In line with the scant luminescence data available for such compounds in the literature,^[13a, 13b] the TCBD derivatives **1-3** and **2'** were found to be totally non-emissive in solution at 25 °C (Table 2). This behavior can be traced back to the fact that their lowest singlet excited state is presently a CT state mostly localized on the TCBD. Indeed, as recently demonstrated by Diederich and Armaroli,^[13c] the latter leads often to rapid non-radiative deactivation by bond twisting motions via so called "twisted intermolecular charge transfer" (TICT) excited states.^[22] In contrast, and unsurprisingly considering the literature on related carbon-rich organic luminophores incorporating fluorenyl fragments,^[10c, 20] a strong fluorescence ($\Phi_{em} \geq 78\%$) was found for the precursor compounds **4-6**. Both the lifetimes, which remain in the ns range, and the observed Stokes shifts (4030, 3320 and 2930 cm^{-1} , respectively) are consistent with reported values for this kind of compound, as is the marked positive solvatochromism found for this emission (see ESI).^[10c]

Table 2. Absorption, CV and Emission Data for **1-6** in CH_2Cl_2 at 25 °C.

Cmpd	Absorption λ (nm) [ϵ ($10^3 \text{ M}^{-1} \text{ cm}^{-1}$)]	λ^{S1} [a] / ΔG_{CT} [b] (eV)	Emission [c,d] λ_{em} (nm) [Φ_{em}]	τ_{em} [e] (ns)
1	274 [24.9], 340 [15.9], 414 [33.9], 489 [25.3]	2.54 / 1.46	/	/
2'	293 [39.9], 349 [43.2], 410 [45.9], 483 [46.1]	2.57 / 1.30	/	/
2	287 [37.2], 340 [21.3], 437 [58.5], 485 [sh, 45.3]	2.56 / 1.39	/	/
3	306 [34.5], 441 [29.0, sh], 512 [40.1]	2.42 / 1.25	/	/
4	302 [32.5], 324 [30.1], 365 [55.1]	/	428 [0.78]	1.5
5	301 [55.1], 390 [126.8]	/	448 [0.85]	1.1
6	301 [35.6], 385 [83.2]	/	434 [0.84]	1.2

[a] Energy of the first allowed absorption. [b] Computed according to eq. 1 (see text). [c] Emission wavelength upon excitation of the lowest absorption peak and associated quantum yield. [d] Fluorescence quantum yield determined relative to quinine bisulfate in 0.5 M H_2SO_4 .^[21] [e] Luminescence lifetime.

We then probed the luminescence of TCBD derivatives **1-3** and **2'** in ethanol glasses at 77 K. Under such conditions, these compounds luminesce (Figure 3a) with quantum yields in the range 6-12% (Table 3), a feature not previously observed with closely related derivatives under similar conditions.^[13b] Then, monitoring their luminescence decay at 77 K reveal a multi-

exponential process requiring at least two time constants to be properly fitted, with lifetimes in the ns range (Table 3). This confirms that fluorescence rather than phosphorescence is observed and indicates the presence of two (or more) emitting species or states in the EtOH glass at 77 K. Note however that even at 77 K, no fine structure is apparent, nor any other diagnostic change in the bandshape of the emission bands that would indicate the existence of several overlapped peaks.

Table 3. Absorption and Emission Data for **1-3** and **2'** in ethanol at 77 K.

Cmpd	Absorption λ (nm)	Emission [a,b] λ_{em} (nm/eV) [Φ_{em}]	τ_{em} (ns) [c]
1	268, 334, 406, 479	664 / 1.86 [0.12]	$\tau_1 = 6.0$ (76%), $\tau_2 = 0.9$ ns (24%)
2'	292, 345, 398, 469	684 / 1.81 [0.11]	$\tau_1 = 5.7$ (61%), $\tau_2 = 1.9$ (39%)
2	279, 337, 419, 474 (sh)	682 / 1.82 [0.08]	$\tau_1 = 5.5$ (61%), $\tau_2 = 0.8$ (39%)
3	301, 419 (sh), 495	696 / 1.81 [0.06]	$\tau_1 = 3.3$ (40%), $\tau_2 = 0.4$ (60%)

[a] Emission wavelength upon excitation at the lowest absorption peak, and associated quantum yield. [b] Fluorescence quantum yield determined against rhodamine 101 in EtOH at 77 K ($\Phi_F = 1$).^[21] [c] Luminescence lifetimes (contributing percentages).

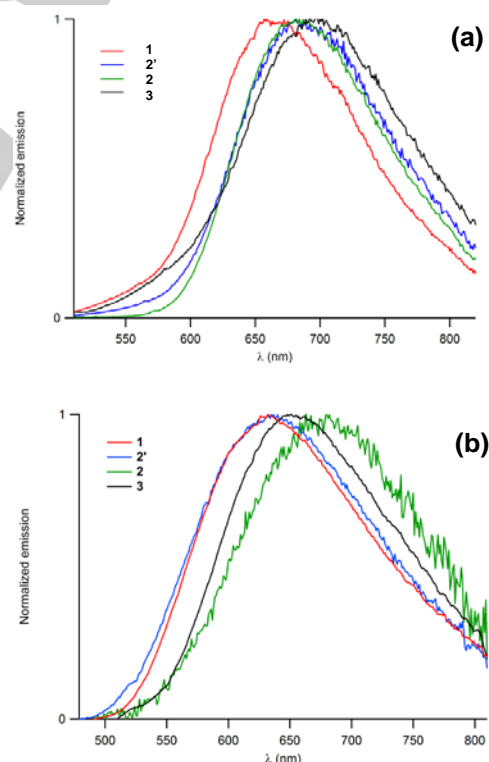


Figure 3. Emission spectra of **1-3** and **2'** in EtOH at 77 K (a) and in SOA glass at 298 K (b)

To find out if the restored fluorescence was attributable to the lower temperature or to the increased viscosity of the medium we next probed the luminescence of **1-3** and **2'** in sucrose octaacetate (SOA) at 298 K, which gives rigid glasses at ambient temperatures.^[23] Again, fluorescence was observed in a close wavelength range for each sample (Figure 3b), but with halved (**1**, **2'**, **3**) or even lower (**2**) quantum yields (Table 4). The hypsochromic shifts observed for both the first absorptions and emissions of all compounds when proceeding from EtOH to SOA glasses (ESI) can easily be rationalized by considering the positive solvatochromism usually observed for such CT transitions along with the lower dielectric constant of SOA relative to EtOH. Indeed, the former is conveniently approximated by that of ethyl acetate.^[23] To the best of our knowledge, the fluorescence quantum yields found for **1-3** and **2'** in SOA glasses are among the largest ones ever reported so far for TCBD derivatives at ambient temperatures.^[13a] The increased rigidity of the surrounding medium must be (at least in part) at the origin of this phenomenon. In line with Amarolli and Diederich's work previously mentioned,^[13c] such a behaviour is often diagnostic of the intermediacy of TICT states during relaxation.^[22, 23] Lifetime measurements further substantiate the strong similarities between the emitting state(s) for a given compound in SOA and EtOH glasses, in spite of the difference in temperature. In both cases, the existence of mainly two emitting species/states in close proportions (compare Table 3 and 4) with different lifetimes but unresolved emission is evidenced. The observation of multi-exponential fluorescence decay for a pure luminophore in SOA has precedence. This phenomenon was previously attributed to the existence of families of conformers „locked“ within the glassy matrix.^[23]

In order to learn more about the nature of the emitting states at room temperature, Stokes shifts and λ_{0-0} values were determined from the spectral data obtained in SOA glasses (ESI). These „apparent“ figures are evidently averaged over the various emitting states and must therefore be considered with caution. First, the Stokes shifts found for **1-3** and **2'** (5054, 5783, 4623 and 5619 cm^{-1} , respectively) are 25-70 % larger than those found for **4-6**. In accordance with the rare examples of fluorescence reported so far for TCBD derivatives in solution,^[13a] these values reveal that a significant structural reorganization takes place during the relaxation process. Then, the λ_{0-0} energies of 2.14-2.27 eV found indicate that the (singlet) emitting state(s) should be ca. 0.9 eV higher in energy than the CT state at lowest energy for which the energies have been derived in CH_2Cl_2 (Table 2). Correcting these energies for the change in polarity between CH_2Cl_2 and SOA only marginally reduces this energy gap ($\Delta G_{\text{CT}} = 1.47$ eV, 1.41 eV, 1.32 eV and 1.40 eV for **1-3** and **2'** in SOA).^[13b] In addition, even the various λ_{em} energies corresponding to the emission maxima in the SOA glasses (Table 4) are ca. 0.5 eV higher than these values. These observations strongly suggest that most of the emitting states (if not all) are significantly higher in energy than the fully relaxed CT state, which likely correspond to the TICT state.^[22b] The present MO calculations (see later) indicate however that these luminescent state(s), likewise to the TICT state, result from an initial $(\pi^*)_{\text{TCNE}} \leftarrow (\pi)_{\text{FluNPr}_2}$ photoinduced charge transfer. Therefore they likely correspond to the (vertical) untwisted CT state. Notably, based on the ΔG_{CT} determined for the various TCBD derivatives in SOA, we also want to stress that the

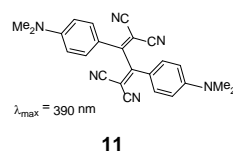
corresponding TICT states should emit in the 850-950 nm region, thus outside the detection range of our fluorimeter.

Table 4. Absorption and Emission Data for **1-3** and **2'** in sucrose octaacetate (SOA) glass at 298 K.

Cmpd	Absorption λ (nm)	Emission ^[a,b] λ_{em} (nm/eV) [Φ_{em}]	τ_{em} (ns) ^[c]
1	325, 405, 479	632 / 1.96 [0.06]	$\tau_1 = 5.3$ (66%), $\tau_2 = 1.6$ ns (34%)
2'	352, 396, 468	635 / 1.95 [0.05]	$\tau_1 = 5.3$ (57%), $\tau_2 = 1.6$ (43%)
2	420, 486 (sh)	676 / 1.83 [0.02]	$\tau_1 = 5.2$ (57%), $\tau_2 = 1.0$ (43%)
3	412, 501	652 / 1.90 [0.06]	$\tau_1 = 5.0$ (64%), $\tau_2 = 1.7$ (36%)

[a] Emission wavelength upon excitation at the lowest absorption peak, and associated quantum yield. [b] Fluorescence quantum yield determined against rhodamine 101 in EtOH ($\Phi_{\text{F}} = 1$).^[21] [c] Luminescence lifetimes (contributing percentages).

Based on present work and on calculations of Diederich and Amarolli,^[13c] we tentatively propose that the radiative relaxation proceeds from the first singlet excited state of **1-3** and **2'**, assuming that it corresponds to the „vertical“ CT state. Relaxation would operate from this state via a twisting motion of one of the aromatic units connected to the TCBD unit. Consistent with this hypothesis, increasing the viscosity of the matrix would restore the fluorescence by slowing down these rotational motions. Relaxation would proceed through the TICT state leading eventually to the GS by back electron transfer, but emission from the TICT state cannot be probed under our experimental conditions. Finally, the photogeneration of two (or more) distinct emissive states likely corresponds to different conformers, rigidly trapped in the solvent glass.

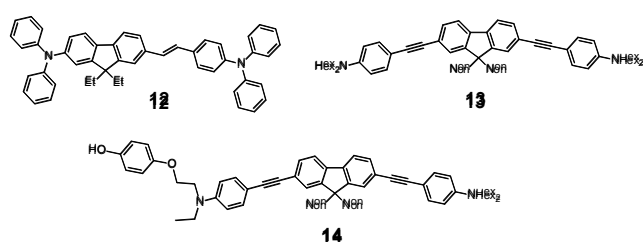


Scheme 3. Quadrupolar TCBD derivative related to **2** and **3**.

A closer look at our data reveals that the most fluorescent species are **1** and **2'** in ethanol glasses at 77 K. When compared to **11** (Scheme 3) which is not fluorescent in solvent glasses at 77 K,^[13b] it appears replacement of one 4-dimethyl-aminophenyl groups in **11** by a less electron-rich aromatic group such as 2-fluorenyl or 2-(7-diphenylamino)fluorenyl and replacement of the remaining dimethylamino unit by the less electron-releasing diphenylamino donor is sufficient to restore some fluorescence in rigid media at room temperature. Considering that the triarylamino donor groups in **1** and **2'** are more bulky and therefore certainly more prone to be influenced by the viscosity of the surrounding medium during relaxation, steric factors might be at the origin of that change. Alternatively, based on CV data ($E^{\circ}_{\text{Ox}} - E^{\circ}_{\text{Red}} = 1.92$ eV in CH_2Cl_2),^[13a] both **1** and **2'** present also apparently lower ΔG_{CT} values than **11**, meaning that a smaller driving force for charge recombination is operative for these

compounds. At this stage, further studies are needed to unambiguously determine if the restored fluorescence of **1-3** and **2'** in solvent glasses can be dominantly attributed to steric or electronic factors.

Two-photon Emission Studies. The 2PA cross-sections (Table 5) at 25 °C were next determined for **4-6** using two-photon excited fluorescence (TPEF). The highest values are found for the quadrupolar derivative **5**, followed by that of the multipolar derivative **6** possessing two distinct diphenylamino donor groups, while the purely dipolar derivative **4** is clearly less active. The 2PA cross-section for **6** is significantly larger than that obtained for its ethynyl analogue **12** by TPEF, for which a value of 282 GM at 730 nm had been reported in toluene solutions.^[20] Surprisingly, ^[10c,7b,9] this suggests that the ethynyl bridge is better than the 1,2-ethynyl unit in promoting 2PA in such compounds.



Scheme 4. Selected two-photon absorbers related to **5** and **6**.

Table 5. 2PA maximal values of **1-6** in dichloromethane at 25 °C determined by TPEF or Z-scan.

Compd /method	$\lambda_{\text{OPA}}^{\text{[a]}}$ (nm)	$\lambda_{2\text{PA}}^{\text{[b]}}$ (nm)	$\sigma_2^{\text{[c]}}$ (GM)	$\sigma_{2,\text{max}}/MW^{\text{[d]}}$ (GM/g)	$\phi, \sigma_2^{\text{[e]}}$ (GM)
1/Z-scan	489	925 ^[f]	115 ^[f]	0.17 ^[f]	/
2/Z-scan	415/488	800/950	170/210	0.16/0.20	/
2'/Z-scan	410/483	850/950	330/310	0.35/0.33	/
3/Z-scan	512	1050	390	0.46	/
4/TPEF	365	750	140	0.27	109
5/TPEF	391	720	980	1.21	833
6/TPEF	385	700	540	0.76	454

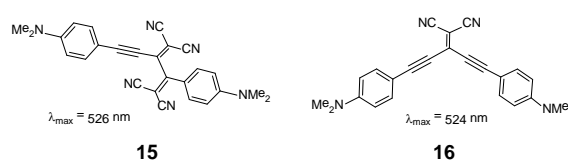
[a] One-photon absorption corresponding to the detected 2PA maximum. [b] Maximal value of the two-photon absorption ($\pm \leq 10\%$). [c] 2PA cross-sections measured by TPEF in the femtosecond regime. TPEF cross-sections were measured relative to fluorescein in 0.01 M aqueous NaOH over the range 715–980 nm,^[17] with the appropriate solvent-related refractive index corrections.^[18] Data points between 700 and 715 nm were corrected according to ref. [10e] [d] Figure-of-merit relevant for applications in optical limiting or nanofabrication.^[9b] [e] Two-photon brightness relevant figure-of-merit for imaging applications.^[19] In these expressions, MW represents the molecular weight and ϕ the luminescence quantum yield. [f] Determined in THF.

For **4**, the match between the absorption maxima in the 2PA and OPA spectra divided by two is excellent (ESI), indicating that 1PA takes place in the lowest one-photon-allowed excited state. In contrast, the 2PA band maximum for **5** is observed at somewhat higher energy than that of the lowest-lying allowed

one-photon absorption divided by two. This can be related to the different selection rules operating for one- and two-photon absorption in this centrosymmetric quadrupolar chromophore, resulting in a larger 2PA cross-section for the one-photon forbidden and two-photon allowed state.^[10c] In line with measurements reported for **12**,^[20] it seems that a somewhat similar situation prevails in the case of the non-centrosymmetric multipolar derivative **6** (ESI), although both excited states should be now one-photon allowed. Notably, **5** performs slightly better than both its dihexylamino / nonyl analogue **13** (Scheme 4)^[10c] and its dissymmetric analogue **14**, while possessing a slight red-shifted absorption maximum (720 nm vs. 703 ± 2 nm for **13** and **14**; see ESI).^[10f] In terms of applications, **4** and **6** are potentially interesting as photoinitiators for nanofabrication, while **5** may be of interest for bioimaging purposes,^[7b] or even optical limiting/rectification in the near-IR range.^[24]

Z-scan Studies. We then examined **1-3** and **2'** by Z-scan in order to determine their cubic nonlinear optical properties. The molecular third-order NLO coefficients of these compounds in the near-IR domain are dominated by their real parts (γ_{Re}) which are overall negative (ESI). Due to dispersion, very large negative peaks are observed near 1250 nm, except for **2'** for which a positive peak is present instead (Table 6). At longer wavelengths, these values converge to negative values of much lower magnitude. Unfortunately, the fairly large experimental uncertainty forbids their accurate evaluation, but their magnitude is in the range previously determined at 1500 nm ($6 \times 10^{-48} \text{ m}^5 \text{ V}^{-2}$ or $43 \times 10^{-35} \text{ esu}$) by four-wave mixing (DFWM) for related polycyano derivatives such as **15** (Scheme 5), at least for **2-3** and **2'**.^[3, 6] When taking into consideration either the number of active electrons^[25] or the molecular mass of the compounds,^[3a] the asymmetric derivative **3** appears to be the most active among **1-3** in the spectral range investigated. Notably, comparison with **1** reveals that inclusion of a second donor site is essential to promote a large cubic NLO activity in the near-IR range.

We next sought to determine their 2PA cross-sections from the open-aperture measurements (Table 5). For **1** and **3**, Z-scan reveals only one maximum in the NIR range which matches with half of the energy of the dominant one-photon peak detected in the visible range, whereas for **2** and **2'** (Figure 4 and ESI), essentially two maxima are revealed which likewise correspond to half of the energy of the strongest one-photon-allowed transitions at lowest energy. For **2** and **2'**, several additional weak 2PA peaks (50–100 GM) can be detected at lower energies. These peaks most likely correspond to excited states at the red edge of the main absorption band with low oscillator strengths. According to previous results and DFT calculations (see later), they probably correspond to excited CT states associated with HOMO-LUMO transitions in more energetic (twisted) conformations. These 2PA values are all larger than that previously reported for the related derivative **16** (88 GM) at 900 nm.^[7a]



Scheme 5. Selected poly-cyano derivatives related to **1-3** for which cubic NLO have been determined.

Thus, among **1-3**, the most active two-photon absorber is the multipolar compound **3**, followed by the non-symmetric compound **2'**. Both perform significantly better than the symmetric compound **2** or the shorter non-symmetric compound **1**. This might be traced back to the preservation of extended π -conjugated segments between donor (diphenylamino) and acceptor (TCBD) sites in **2'** and **3**. Indeed, replacement of alkyne spacer by TCBD units, while multiplying the possible intramolecular CT pathways also disrupts π -conjugation between the two sides of the molecule. When compared with 2PA data obtained for **4-6** by TPEF, the 2PA cross-section maximal values for **1-3** and **2'** are lower than those of their precursors, revealing that the inclusion of the TCBD unit in these structures is actually detrimental to their two-photon cross-sections.^[27] Moreover, a clear loss of transparency in the visible range occurs upon progressing from **4-6** to **1-3** and **2'**, which originates from the numerous low-energy CT excited-states generated by insertion of TCNE in the alkyne spacer.

Table 6. Selected third-order NLO data for **1-3** and **2'** determined in dichloromethane at 25 °C by Z-scan.

Cmpd	λ at $\gamma_{\text{max}}^{[a]}$ (nm)	N ^[b]	$(\gamma_{\text{re}})_{\text{max}}^{[c]}$ (10^{-36} esu)	$ \gamma_{\text{max}} /1400^{[d]}$ (10^{-36} esu)	$\gamma_{\text{max}}/MW^{[e]}$ (10^{-36} esu/g)
1 ^[f]	1100	23.2	-394 ± 35	385 ± 55	0.6
2	1250	31.8	-15100 ± 410	15100 ± 450	14.1
2'	1250	31.0	13900 ± 290	13900 ± 310	14.8
3	1250	24.7	-13500 ± 200	13500 ± 200	16.1

a) Wavelength of the maximal value of γ_{re} in the near-IR range. [b] Number of active π -electrons. [25-26] [c] Minimal value of the real part of γ in the 800-1600 nm range, as determined from closed-aperture Z-scan measurements. [d] Maximum γ value derived. [e] Specific γ value, MW represents the molecular weight. [f] Determined in THF.

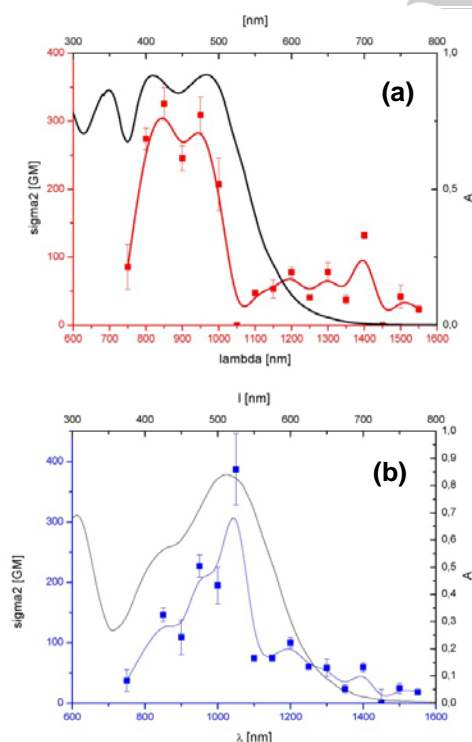


Figure 4. Overlay of one and two-photon absorption spectra for **2'** (a) and **3** (b) in CH_2Cl_2 at 25 °C. The two-photon cross-sections are derived from open-aperture Z-scan measurements and the one-photon spectra are plotted against twice the wavelength (2λ).

In terms of applications,^[28] their overall good third-order activity and sizeable 2PA activity make them suited for applications such as optical-limiting in the near-IR range,^[29] beam re-shaping in the far IR range and evidently for applications not related to their transparency, such as two-photon sensitization for nanolithography or photodynamic therapy.^[7b] Furthermore, compared to other purely organic structures envisioned for such applications, their remarkable redox activity constitutes an additional and important key feature which might open new opportunities for using them in electro-optic devices in the future.^[30]

DFT Calculations. The compounds were modeled using DFT on simplified models without the butyl chains on fluorenyl (**C1-C6**). To assist attribution of the IR and UV-vis absorption spectra recorded for **1-6**, modelling of the IR absorptions was performed for **C1-C6**, as well as TD-DFT calculations. Once scaled using the proper factor to correct for anisotropy (0.951),^[31] the computed vibrational spectra reproduced satisfyingly (see Supporting Information) the most characteristic vibrational modes of **1-6** and helped us in the assignment of the characteristic stretching modes of these molecules, while TD-DFT calculations reproduced the experimentally observed spectra within 0.3 eV (Table 7).

As expected, the match is less satisfactory for electronic transitions involving long-range charge transfer when employing such a functional which does not incorporate long-range corrections.^[32] The calculations are nevertheless sufficient to provide a qualitative understanding of the origin of the excited states underlying the absorptions of **1-3**. Furthermore, we verified in selected cases that the observed discrepancies do not originate from different conformers than the ones computed, a distribution of these being certainly present in solution. Indeed, a nearly similar spectral shape was obtained in each case for various low-energy rotamers of the TCBD single bonds modeled by TD-DFT (see ESI).

For **C1-C3**, the HOMO is mostly located on the triphenylamino fragment and the LUMO-1 either on the fluorenyl fragment (**C1**) or on the triphenylamino fragments (**C2-C3**), whereas the HOMO and LUMO+1 are strongly located on the TCBD fragment(s). In line with our CV data (Table 1), calculations thus confirm that an electron mostly located on the triphenylamino group will be ionized first upon oxidation, whereas reduction will result in injection of an electron into the π^* of the TCBD units. Unsurprisingly, the allowed (singlet-singlet) transitions are LUMO \leftarrow HOMO and have a strong CT character in **1-3**, as briefly mentioned above (Table 6). The next lowest-energy transitions in these derivatives apparently involve transitions more localized on the fluorenyl or triphenylamino fragments.

Regarding their alkynyl precursors (**C4-C6**), the HOMO is also strongly localized on the triphenylamino fragment, while the LUMO is a π^* MO on the fluorenyl and alkynyl ligand(s). Thus, the first allowed transition at lowest energy is a $\pi^* \leftarrow \pi$ transition with some CT character (ESI, Table S4). Again, the next lowest-energy transitions in these derivatives apparently involve

transitions more localized on the fluorenyl or triphenylamino fragments.

Note that the calculated transition moments for the (long range) CT transitions at lowest energy are somewhat overestimated, as is sometime the case for long-range charge transfer.^[32] As a result, the red-side of the simulated spectra is slightly more intense than experimentally observed, especially for **2'** and **3**. The existence of poorly allowed CT transitions on the red side of the main absorption peak observed in the 600-700 nm spectral range is also attested by the presence of sizeable 2PA in the 1200-1400 nm range. In line with literature,^[1, 13c] calculations indicate that these will correspond to excitations from the most electropositive triphenylamino donor toward the TCBD acceptor(s), but for molecules having more energetic conformations than the GS one.

Table 7. Experimental vs. Computed ^[a] (PBE0 / 6-31G) Values (nm). Energy and Composition of the First Singlet Excited States (Wavelength, Oscillator Strength *f*, Transition Percentage)

Cmpd	Experimental λ_{\max} [ϵ] ^[b]	Calculated ^[c] λ_{\max} [<i>f</i>] ^[d]	Composition	Major Assignment ^[e]	
1		544 [0.16]	154 → 155 (96%)	(π^*)TCNE ← (π)PhNPh ₂	
	489 [25.3]	432 [0.26]	153 → 155 (94%)	(π^*)TCNE ← (π)Flu	
	414 [33.9]	418 [0.54]	154 → 156 (92%)	(π^*)Flu/TCNE ← (π)PhNPh ₂	
	340 [15.9]	358 [0.42]	153 → 156 (92%)	(π^*)Flu/TCNE ← (π)Flu	
	274 [24.9]	280 [0.14]	154 → 160 (62%)	(π^*)Flu ← (π)PhNPh ₂	
	2	/	599 [0.11]	256 → 257 (87%)	(π^*)TCNE/Flu ← (π)PhNPh ₂
		485 [45.3]	499 [0.12]	256 → 258 (88%)	(π^*)TCNE ← (π)PhNPh ₂
		437 [58.5]	437 [1.02]	254 → 257 (82%)	(π^*)TCNE/Flu ← (π)Flu
		/	422 [0.56]	255 → 259 (86%)	(π^*)TCNE/Flu ← (π)PhNPh ₂
		340 [21.3]	383 [0.12]	255 → 260 (80%)	(π^*)TCNE ← (π)PhNPh ₂
/		359 [0.11]	253 → 257 (71%)	(π^*)TCNE/Flu ← (π)PhNPh ₂	
287 [37.2]		288 [0.11]	252 → 259 (51%)	(π^*)TCNE/Flu ← (π)PhNPh ₂	
/		277 [0.10]	244 → 258 (63%)	(π^*)TCNE ← (π)NPh ₂	
2'			647 [0.32]	224 → 225 (99%)	(π^*)TCNE ← (π)NPh ₃
			549 [0.17]	223 → 225 (96%)	(π^*)TCNE ← (π)NPh ₃
	483 [46.1]	488 [0.42]	224 → 226 (96%)	(π^*)TCNE/Flu ← (π)NPh ₃	
	/	456 [0.38]	222 → 225 (π^*)TCNE		

				(94%)	← (π)Flu/NPh ₃
	410 [45.9]	419 [0.55]	223 → 226 (93%)	(π^*)TCNE/Flu ← (π)NPh ₃	
		377 [0.83]	222 → 226 (69%)	(π^*)TCNE/Flu ← (π)Flu/NPh ₃	
	349 [43.2]	366 [0.36]	224 → 227 (66%)	(π^*)Flu ← (π)NPh ₃	
	293 [39.9]	299 [0.16]	224 → 233 (80%)	(π^*)NPh ₂ ← (π)NPh ₃	
		291 [0.17]	222 → 227 (52%)	(π^*)Flu ← (π)Flu/NPh ₃	
3		512 [40.1]	606 [0.32]	198 → 199 (99%)	(π^*)TCNE ← (π)NPh ₃
			533 [0.16]	197 → 199 (96%)	(π^*)TCNE ← (π)NPh ₃
		441 [29.0, sh]	473 [0.38]	198 → 200 (96%)	(π^*)TCNE/Flu ← (π)NPh ₃
		/	418 [0.54]	197 → 200 (94%)	(π^*)TCNE ← (π)Flu/NPh ₂
			387 [0.17]	196 → 199 (94%)	(π^*)TCNE/Flu ← (π)Flu/NPh ₂
			333 [0.15]	196 → 200 (42%)	(π^*)TCNE/Flu ← (π)Flu/NPh ₂
				193 → 199 (21%)	(π^*)TCNE ← (π)PhNPh ₂
		306 [34.5]	327 [0.15]	195 → 199 (36%)	(π^*)TCNE ← (π)PhNPh ₂
			296 [0.15]	198 → 205 (67%)	(π^*)NPh ₂ ← (π)Flu/NPh ₂

[a] The calculated excited states are ¹A. [b] Experimental absorption (nm) and extinction coefficients (ϵ) in $10^3 \text{ M}^{-1} \cdot \text{cm}^{-1}$. [c] in nm. [d] Computed transition moment under vacuum. [e] See ESI for the plot of the corresponding MOs.

Conclusions

We have reported here the synthesis and characterization of four new TCBD derivatives (**1-3** and **2'**) featuring fluorenyl and triaryl amino groups. While exhibiting the characteristic electroactivity expected for TCBDs and triaryl amino-containing derivatives, we show here that none of these multipolar derivatives are fluorescent in solution at ambient temperatures, in contrast to their alkyne precursors (**4-6**). However, **1-3** and **2'** were shown to be fluorescent in solvent glasses. This unprecedented finding is important, since it potentially opens an access to fluorescent materials by embedding these derivatives in rigid matrixes. The 2PA properties of these conjugated derivatives have been investigated by TPEF or Z-scan and it was shown that **1-3** and **2'** are two-photon absorbers into their lowest excited states, **3** being the most active among them. 2PA takes place deep in the near-IR range, but their cross-sections are lower than for their corresponding precursors (**4-6**), in line

with the diminished fluorenyl character of the corresponding excited states. Thus, cycloaddition of TCNE at **4-6** constitutes a simple means to shift both the linear and nonlinear absorption maxima to lower energies. The refractive third-order NLO properties of **1-3** and **2'** have also been investigated. Similar to the few TCBD derivatives previously investigated, the fair cubic NLO activities in the near-IR range make them worth consideration for various applications in the near/far-IR range, such as optical limiting, pulse re-shaping or two-photon photosensitization. Furthermore, the remarkable redox-activity of these all-organic structures combined with their specific cubic NLO activity in the near-IR range might open new opportunities for their applied use in the future.

In terms of molecular design, the present study suggests that third-order NLO properties might be even more favored in related derivatives presenting an extended and electron-rich π -manifold on the external fluorenyl side, while luminescence seem to be favored in derivatives lacking a second amino group on this part, such as **1**, or having it further removed from TCBD core, such as in **2'**. Also, keeping an overall centrosymmetry, such as in **2**, does apparently not constitute a decisive structural feature for improving further these properties.

Experimental Section

General. All reactions and work-up procedures of air-sensitive compounds were carried out under dry, high-purity argon or nitrogen, using standard Schlenk techniques.^[33] All glassware was oven-dried overnight at 120 °C prior to use. Solvents/reagents were dried and distilled as follows: Et₂O, hexane and reagent grade THF (sodium-benzophenone), CH₂Cl₂ (CaH₂), diisopropylamine and triethylamine (KOH), and DMF (activated 3 Å molecular sieves). Flash column chromatography was performed using silica (Acros 60 Å, 40-60 mesh). Hexane used for column chromatography refers to petroleum spirit (boiling point range 60-80 °C). *p*-(HC=CC₆H₄)NPh₂, (**7**)^[17, 34] and 2,7-diodo-9,9-dibutylfluorene (**9**)^[12, 35] were obtained as described in the literature. Other chemicals were purchased from a commercial source (Sigma-Aldrich) and used as received.

Instrumentation. Melting points were taken in air using a melting point apparatus. Infrared spectra were obtained as KBr disks in the 400-4000 cm⁻¹ range. Raman spectra were obtained from the solid samples by diffuse scattering in the 100-3300 cm⁻¹ range (Stokes emission) with a laser excitation source at 1064 nm (30 mW), using a quartz separator with a FRA 106 detector. NMR spectra were acquired at 298 K on 400 and/or 500 MHz FT NMR spectrometers. Cyclic voltammograms were recorded in dry CH₂Cl₂ solutions (containing 0.1 M [N^oBu₄][PF₆], purged with nitrogen and maintained under an inert atmosphere) using a Pt disk as working electrode, a Pt wire as counter electrode and a SCE reference electrode; the FeCp₂^{0/+1} couple (E_{1/2}: 0.46 V,^[36] ΔE_p = 0.09 V; I_{pa}/I_{pc} = 1) was used as an internal calibrant. UV-visible-NIR spectra were recorded using a 1 cm quartz cell on a Cary 5 spectrometer, and are reported as λ_{max} (nm) [log ε (M⁻¹ cm⁻¹)]. Elemental analysis and unit- and high-resolution mass spectra (EI and ESI) were obtained at the Centre Regional de Mesures Physiques de l'Ouest (CRMPO) or at Wrocław University of Technology (WUT).

Synthesis of compound 1: A solution of the fluorene derivative **4** (61 mg, 0.11 mmol) and TCNE (14 mg, 0.11 mmol) in CH₂Cl₂ (1.1 mL) was stirred at 20 °C for 15 h. The reaction mixture was concentrated under reduced pressure to give the title compound (75 mg, 100%) as a dark red solid. **MP:** 108-111 °C. **R_f:** 0.24 [Petroleum ether/Et₂O (9:1)]. **¹H NMR** (400 MHz, CDCl₃) δ = 7.83 (1H, d, *J* = 1.5 Hz, H_{F1u}), 7.72 (1H, d, *J* = 8.1 Hz, H_{F1u}), 7.71-7.67 (1H, m, H_{F1u}), 7.61 (2H, d, *J* = 9.3 Hz, H_{Ar}), 7.46 (1H, dd, *J* = 1.9 and 8.1 Hz, H_{F1u}), 7.39-7.28 (7H, m, H_{Ar} and 3H_{F1u}), 7.21-

7.11 (6H, m, 2H_{Ar}), 6.86 (2H, d, *J* = 9.3 Hz, H_{Ar}), 2.03-1.85 (4H, m, H_{Bu}), 1.05-0.92 (4H, m, H_{Bu}), 0.57 (6H, t, *J* = 7.3 Hz, H_{Bu}), 0.54-0.44 (4H, m, H_{Bu}). **¹³C{¹H} NMR** (100 MHz, CDCl₃) δ = 168.9, 164.7, 153.8, 152.6, 152.3, 148.2, 144.7, 130.3, 132.1, 130.3, 130.2, 129.9, 129.4, 127.6, 127.1, 126.8, 124.5, 123.4, 122.0, 121.4, 121.0, 118.2, 113.8, 112.8, 112.8, 111.9, 85.1, 78.6, 55.8, 39.9, 26.1, 23.0, 13.9. **IR** (KBr, cm⁻¹): ν = 3061, 2928 (m, C_{Ar}-H), 2219 (m, C≡N), 1607 (m, C=C), 1586 (s, C=C_{Ar}). **Raman** (neat, cm⁻¹): ν = 3066 (vw, C_{Ar}-H), 2221 (s, C≡N), 1609 (s, C=C), 1520 (vs, C=C_{Ar}). **HRMS:** calculated for C₄₇H₄₀N₅ [M+H]⁺ 674.32837, found 674.3278, calculated for C₄₇H₃₉N₅ M⁺ 673.32055, found 673.3197. **UV-vis** (CH₂Cl₂): λ_{max} (log ε) = 274 (4.40), 340 (4.20), 414 (4.53), 489 (4.40).

Synthesis of compound 2: A solution of the fluorene derivative **5** (67 mg, 0.083 mmol) and TCNE (21 mg, 0.165 mmol) in CH₂Cl₂ (0.8 mL) was stirred at 20 °C for 16 h. The reaction mixture was purified by column chromatography [Petroleum ether/EtOAc (9:1) to (7:3)] to give TCBD **2** (84 mg, 95%) as a dark red solid. **MP:** decomposition observed above 155 °C. **R_f:** 0.48 [Petroleum ether/EtOAc (4:1)]. **¹H NMR** (400 MHz, CDCl₃): δ = 7.93 (2H, d, *J* = 1.7 Hz, H_{F1u}), 7.89 (2H, d, *J* = 8.1 Hz, H_{F1u}), 7.70 (4H, d, *J* = 9.3 Hz, H_{Ar}), 7.57 (2H, dd, *J* = 1.7 and 8.1 Hz, H_{F1u}), 7.45-7.37 (8H, m, H_{Ar}), 7.32-7.20 (12H, m, H_{Ar}), 6.96 (4H, d, *J* = 9.3 Hz, H_{Ar}), 2.15-2.00 (4H, m, H_{Bu}), 1.13-1.00 (4H, m, H_{Bu}), 0.64 (6H, t, *J* = 7.3 Hz, H_{Bu}), 0.61-0.50 (4H, m, H_{Bu}). **¹³C{¹H} NMR** (100 MHz, CDCl₃): δ = 168.3, 163.6, 153.8, 153.4, 144.8, 144.3, 132.2, 131.9, 130.0, 129.2, 126.9, 126.8, 124.6, 122.3, 121.3, 117.9, 113.6, 112.8, 112.2, 111.4, 87.0, 78.0, 56.4, 39.3, 25.9, 22.7, 13.7. **IR** (KBr, cm⁻¹): ν = 3036 (m, C_{Ar}-H), 2928 (m, C_{Ar}-H), 2220 (m, C≡N), 1608 (s, C=C), 1586 (s, C=C_{Ar}). **Raman** (neat, cm⁻¹): ν = 3067 (vw, C_{Ar}-H), 2222 (s, C≡N), 1610 (s, C=C), 1522 (vs, C=C_{Ar}). **HRMS:** calculated for C₇₃H₅₃N₁₀ [M+H]⁺ 1069.44492, found 1069.4440, calculated for C₇₃H₅₂N₁₀ M⁺ 1068.43764, found 1068.4377. **UV-vis** (CH₂Cl₂): λ_{max} (log ε) = 287 (5.57), 340 (4.32), 437 (4.76), 485 (4.65).

Synthesis of compound 2': A solution of the fluorene derivative **5** (68 mg, 0.084 mmol) and TCNE (11 mg, 0.084 mmol) in CH₂Cl₂ (0.8 mL) was stirred at 20 °C for 16 h. The reaction mixture was purified by column chromatography [Petroleum ether/EtOAc (1:0) to (7:3)] to give the title compound (48 mg, 61%) and compound **2** (17 mg, 19%) as dark red solids. **MP:** 135-138 °C. **R_f:** 0.92 [Petroleum ether/EtOAc (4:1)]. **¹H NMR** (400 MHz, CDCl₃): δ = 7.83 (1H, d, *J* = 1.6 Hz, H_{F1u}), 7.70-7.71 (1H, d, *J* = 8.1 Hz, H_{F1u}), 7.64 (1H, dd, *J* = 0.8 and 7.7 Hz, H_{F1u}), 7.61 (2H, d, *J* = 9.3 Hz, H_{Ar}), 7.48-7.46 (1H, m, H_{F1u}), 7.44 (2H, br s, H_{F1u}), 7.36-7.28 (6H, m, H_{Ar} and H_{F1u}), 7.24-7.11 (10H, m, 3H_{Ar}), 7.07-7.03 (4H, m, H_{Ar}), 7.00 (2H, tt, *J* = 1.1 and 7.3 Hz, H_{Ar}), 6.94 (2H, d, *J* = 8.8 Hz, H_{Ar}), 6.86 (2H, d, *J* = 9.3 Hz, H_{Ar}), 2.03-1.85 (4H, m, H_{Bu}), 1.05-0.94 (4H, m, H_{Bu}), 0.58 (6H, t, *J* = 7.3 Hz, H_{Bu}), 0.55-0.39 (4H, m, H_{Bu}). **¹³C{¹H} NMR** (100 MHz, CDCl₃): δ = 168.6, 164.5, 153.8, 152.6, 152.5, 148.3, 147.3, 147.2, 144.6, 138.6, 132.7, 132.0, 131.1, 130.5, 130.2, 129.5, 129.4, 127.0, 126.8, 126.1, 125.2, 124.9, 124.4, 123.8, 122.1, 122.0, 121.3, 121.1, 118.1, 115.6, 113.7, 112.8, 112.7, 111.9, 91.9, 89.4, 85.2, 78.5, 55.8, 39.8, 26.0, 23.0, 13.9. **IR** (KBr, cm⁻¹): ν = 3036 (m, C_{Ar}-H), 2928 (m, C_{Ar}-H), 2221 (m, C≡N), 2195 (vw, C≡C), 1606 (s, C=C), 1586 (s, C=C_{Ar}). **Raman** (neat, cm⁻¹): ν = 3065 (vw, C_{Ar}-H), 2222 (s, C≡N), 2199 (s, C=C), 1609 (vs, C=C), 1523 (s, C=C_{Ar}). **HRMS:** calculated for C₆₇H₅₃N₆ [M+H]⁺ 941.43262, found 941.4325, calculated for C₆₇H₅₂N₆ M⁺ 940.42535, found 940.4258. **UV-vis** (CH₂Cl₂): λ_{max} (log ε) = 293 (4.60), 348 (4.64), 409 (4.66), 483 (4.66) nm.

Synthesis of compound 3: A solution of the fluorene derivative **6** (65 mg, 0.091 mmol) and TCNE (12 mg, 0.091 mmol) in CH₂Cl₂ (0.9 mL) was stirred at 20 °C for 16 h. The reaction mixture was purified by column chromatography [Petroleum ether/Et₂O (1:0) to (3:2)] to give the title compound (73 mg, 95%) as a dark fushia solid. **MP:** 108-110 °C. **R_f:** 0.20 [Petroleum ether/Et₂O (4:1)]. **¹H NMR** (400 MHz, CDCl₃): δ = 7.92 (1H, d, *J* = 1.5 Hz, H_{F1u}), 7.75 (2H, d, *J* = 9.2 Hz, H_{Ar}), 7.71 (1H, d, *J* = 8.2 Hz, H_{F1u}), 7.65-7.57 (2H, m, 2H_{F1u}), 7.43 (4H, t, *J* = 7.8 Hz, H_{Ar}), 7.37-7.24 (10H, m, 2H_{Ar} and H_{F1u}), 7.20 (4H, d, *J* = 7.6 Hz, H_{Ar}), 7.14 (3H, m, 2H_{Ar}), 7.12-7.05 (1H, m, H_{F1u}), 7.00 (2H, d, *J* = 9.2 Hz, H_{Ar}), 2.07-1.83 (4H, m,

H_{Bu}), 1.19-1.06 (4H, m, H_{Bu}), 0.75 (6H, t, J 7.3 Hz, H_{Bu}), 0.72-0.63 (4H, m, H_{Bu}). $^{13}C\{^1H\}$ NMR (100 MHz, $CDCl_3$): δ = 168.3, 165.0, 154.3, 153.7, 151.9, 150.0, 148.3, 147.4, 144.6, 132.9, 132.0, 130.2, 129.8, 129.5, 129.1, 127.0, 126.7, 125.0, 124.1, 123.8, 122.2, 122.1, 120.0, 118.1, 117.2, 113.8, 113.1, 112.8, 112.2, 83.4, 78.6, 55.5, 39.6, 26.1, 22.9, 13.9. IR (KBr, cm^{-1}): ν = 3036 (m, C_{Ar-H}), 2928 (m, C_{Ar-H}), 2221 (vw, $C\equiv N$), 1605 (s, $C=C$), 1587 (s, $C=C_{Ar}$). Raman (neat, cm^{-1}): ν = 3065 (vw, C_{Ar-H}), 2223 (s, $C\equiv N$), 1603 (s, $C=C$), 1522 (vs, $C=C_{Ar}$). HRMS: calculated for $C_{59}H_{49}N_6$ [$M+H$] $^+$ 841.40187, found 841.4011, calculated for $C_{47}H_{39}N_5$ M^+ 840.39405, found 840.3942. UV-vis (CH_2Cl_2): λ_{max} (log ϵ) = 306 (4.54), 417 sh (4.44), 512 (4.62) nm.

Synthesis of 2-(4-diphenylamino-1-phenylethynyl)-9,9-dibutylfluorene (4): To a flask under argon were added 2-bromo-9,9-dibutylfluorene (**8**; 1.05 g, 2.99 mmol, 1 eq.), *N*-(4-phenylethynyl)-*N,N*-diphenylamine (**7**; 0.87 g, 3.23 mmol, 1.1 eq.), CuI (27 mg, 0.15 mmol, 0.05 eq.), and Pd(PPh_3) $_2Cl_2$ (105 mg, 0.15 mmol, 0.05 eq.). Toluene (20 mL) and diisopropylamine (5 mL) were subsequently added. The colour of the reaction medium changed from orange to black. After stirring 12 h at 25 °C, the solvents were evaporated and the resulting dark solid was dissolved in CH_2Cl_2 (20 mL) and passed through a Celite pad. After evaporation of the solvent, the solid was washed with water and brine, dried in vacuum, and purified by flash chromatography using hexane/ CH_2Cl_2 (7:3) mixtures, to afford the title compound as a pale yellow solid (1.372 g, 52%). MP: 141-142 °C. R_f : 0.44 [hexane/ CH_2Cl_2 (7:3)]. 1H -NMR (400 MHz, $CDCl_3$): δ = 7.68-7.77 (m, 2H, H_{Ar}), 7.48 (d, J = 8.4 Hz, 2H, H_{Ar}), 7.56 (m, 2H, H_{Ar}), 7.29-7.42 (m, 7H, H_{Ar}), 7.19 (d, J = 7.9 Hz, 4H, H_{Ar}), 7.1 (m, 4H, H_{Ar}), 2.04 (t, J = 8.2 Hz, 4H, H_{Bu}), 1.05-1.22 (m, 4H, H_{Bu}), 0.73 (t, J = 7.3 Hz, 6H, H_{Bu}), 0.60-0.90 (m, 4H, H_{Bu}). $^{13}C\{^1H\}$ -NMR (100 MHz, $CDCl_3$): δ = 151.0, 150.7, 147.9, 147.3, 141.2, 140.5, 132.5, 130.5, 129.4, 127.4, 126.9, 125.8, 125.0, 123.5, 122.9, 122.4, 121.8, 119.9, 119.6, 116.3, 89.8, 89.7, 55.1, 40.2, 25.9, 23.1, 13.8. IR (KBr, cm^{-1}): ν = 3036 (m, C_{Ar-H}), 2925 (m, C_{Ar-H}), 2197 (vw, $C\equiv C$), 1590 (s, $C=C_{Ar}$). Raman (neat, cm^{-1}): ν = 2200 (s, $C\equiv C$), 1620 (vs, $C=C_{Ar}$). HRMS: calc. for $C_{41}H_{39}N$: 545.3083 [M] $^+$, found 545.3087. UV-vis (CH_2Cl_2): λ_{max} (log ϵ) = 302 (4.51), 324 (4.47), 365 (4.74).

Synthesis of 2,7-bis(4-diphenylamino-1-phenylethynyl)-9,9-dibutylfluorene (5): To a flask under argon were added 2,7-diodo-9,9-dibutylfluorene (**9**; 1.22 g, 2.30 mmol, 1 eq.), *N*-(4-phenylethynyl)-*N,N*-diphenylamine (**7**; 1.36 g, 5.06 mmol, 2.2 eq.), CuI (21.8 mg, 0.115 mmol, 0.05 eq.), and Pd(PPh_3) $_2Cl_2$ (81 mg, 0.115 mmol, 0.05 eq.). Toluene (20 mL) and diisopropylamine (5 mL) were subsequently added. The colour of the reaction medium changed from orange to orange-brown. After stirring 1 h at 25 °C, an orange precipitate was formed. The mixture was further heated 12 h at 80 °C. Solvents were evaporated and the remaining solid was dissolved in CH_2Cl_2 (20 mL) and passed through a short plug of Celite before being washed with a saturated solution of NH_4Cl and with brine. After drying and evaporation, the resulting yellow solid was purified by flash chromatography using hexane/ CH_2Cl_2 (8:2) mixtures, providing the title compound as a golden yellow solid (1.435 g, 77%). MP: 273-275 °C (Dec). R_f : 0.30 (hexane/ CH_2Cl_2 [8:2]). 1H -NMR (400 MHz, $CDCl_3$): δ = 7.65 (d, J = 7.7 Hz, 2H, H_{Ar}), 7.46-7.53 (m, 4H, H_{Ar}), 7.41 (d, J = 7.9 Hz, 4H, H_{Ar}), 7.32-7.23 (m, 8H, H_{Ar}), 7.13 (d, J = 7.9 Hz, 8H, H_{Ar}), 6.96-7.10 (m, 8H, H_{Ar}), 1.82-2.06 (m, 4H, H_{Bu}), 1.00-1.15 (m, 4H, H_{Bu}), 0.68 (t, J = 7.2 Hz, 6H, H_{Bu}), 0.5-0.65 (m, 4H, H_{Bu}). $^{13}C\{^1H\}$ -NMR (100 MHz, $CDCl_3$): δ = 151.1, 147.9, 147.2, 140.5, 132.5, 130.6, 129.4, 125.8, 125.0, 123.6, 122.3, 122.2, 119.9, 116.2, 90.1, 89.7, 55.1, 40.3, 25.9, 23.1, 13.9. HRMS: calc. for $C_{61}H_{52}N_2$: 812.4130 [M] $^+$, found 812.4140. IR (KBr, cm^{-1}): ν = 3034 (m, C_{Ar-H}), 2927 (m, C_{Ar-H}), 2194 (vw, $C\equiv C$), 1590 (s, $C_{Ar=C_{Ar}}$). Raman (neat, cm^{-1}): ν = 2197 (s, $C\equiv C$), 1608 (vs, $C=C_{Ar}$). UV-vis (CH_2Cl_2): λ_{max} (log ϵ) = 301 (4.74), 390 (5.10).

Synthesis of 2-(4-diphenylamino-1-phenylethynyl)-7-diphenylamino-9,9-dibutylfluorene (6): To a flask under argon were added 2-iodo-7-diphenylamino-9,9-dibutylfluorene (**10**; 0.735 g, 1.28 mmol, 1 eq.), *N*-(4-phenylethynyl)-*N,N*-diphenylamine (**7**; 0.414 g, 1.54 mmol, 1.2 eq.), CuI (12 mg, 0.64 mmol, 0.05 eq.), and Pd(PPh_3) $_2Cl_2$ (45 mg, 0.64 mmol, 0.05 eq.). Toluene (20 mL) and diisopropylamine (5 mL) were subsequently

added. The colour of the reaction medium changed from orange to brown. After stirring 12 h at 60 °C, the solvents were evaporated and the resulting dark brown solid was dissolved in CH_2Cl_2 (20 mL) and passed through a Celite pad. After evaporation of the solvent, the solid was washed with water and brine, dried in vacuum, and purified by flash chromatography using hexane/ CH_2Cl_2 (7:3) mixtures to afford the title compound, as a yellow solid (0.671 g, 73%). MP: 217-218 °C (Dec). R_f : 0.32 (hexane/ CH_2Cl_2 [7:3]). 1H -NMR (400 MHz, $CDCl_3$): δ = 7.56 (t, J = 8.5 Hz, 2H, H_{Ar}), 7.49-7.36 (m, 4H, H_{Ar}), 7.32-7.21 (m, 12H, H_{Ar}), 7.16-6.93 (m, 16H, H_{Ar}), 1.94-1.78 (m, 4H, H_{Bu}), 1.15-1.01 (m, 4H, H_{Bu}), 0.71 (t, J = 7.3 Hz, 6H, H_{Bu}), 0.68-0.55 (m, 4H, H_{Bu}). $^{13}C\{^1H\}$ -NMR (100 MHz, $CDCl_3$): δ = 152.5, 150.6, 147.9, 147.8, 147.5, 147.3, 141.0, 135.6, 133.4, 132.5, 130.6, 129.5, 129.4, 129.2, 125.7, 125.3, 125.0, 124.0, 123.5, 123.4, 122.7, 122.4, 121.6, 120.9, 120.6, 119.1, 119.0, 116.4, 89.9, 89.5, 55.0, 40.0, 26.0, 23.0, 13.9. HRMS: calc. for $C_{53}H_{48}N_2$: 712.3817 [M] $^+$, found 712.3820. IR (KBr, cm^{-1}): ν = 3033 (m, C_{Ar-H}), 2927 (m, C_{Ar-H}), 2197 (vw, $C\equiv C$), 1590 (s, $C=C_{Ar}$). Raman (neat, cm^{-1}): ν = 2202 (s, $C\equiv C$), 1603 (vs, $C=C_{Ar}$). UV-vis (CH_2Cl_2): λ_{max} (log ϵ) = 301 (4.55), 385 (4.92).

Synthesis of 2-iodo-7-diphenylamino-9,9-dibutylfluorene (10): Metallic Cu (0.65g, 10.4 mmol, 1.1 eq.) was activated by vigorous stirring in a 2% solution of I_2 in acetone for 15-20 min, followed by stirring in an acidic (30% HCl) acetone solution for 20 min before being separated and dried under vacuum. This sample was subsequently mixed (in the solid state) with 2,7-diodo-9,9-dibutylfluorene (**9**; 5.00 g, 9.4 mmol, 1 eq.), diphenylamine (1.56 g, 9.4 mmol, 1 eq.), K_2CO_3 (3.77g, 27.4 mmol, 2.9 eq.), and 18-crown-6 (0.62 g, 2.0 mmol, 0.25 eq.) in deoxygenated 1,2-dichlorobenzene and heated to 175 °C for 48 h. The reaction mixture was then filtered through a Celite plug and washed with a saturated solution of NH_4Cl until the washings remained colourless. The suspension was then filtered and the solvent evaporated. After drying, the title compound was obtained after purification by flash chromatography, eluting with hexane/ CH_2Cl_2 (9:1) mixtures, as a tan solid (0.776 g, 15%). MP: 122-123 °C. R_f : 0.38 (hexane/ CH_2Cl_2 [9:1]). 1H -NMR (400 MHz, $CDCl_3$): δ = 7.61-7.67 (m, 2H, H_{Ar}), 7.56 (d, J = 8.2 Hz, 1H, H_{Ar}), 7.39 (d, J = 8.3 Hz, 1H, H_{Ar}), 7.29 (t^3 , J = 7.7 Hz, 4H, H_{Ph}), 7.22-7.10 (m, 5H, H_{Ar}), 7.08-7.02 (m, 3H, H_{Ar}), 1.87 (m, 4H, H_{Bu}), 1.04-1.19 (m, 4H, H_{Bu}), 0.75 (t, J = 7.3 Hz, 6H, H_{Bu}), 0.61-0.71 (m, 4H, H_{Bu}). $^{13}C\{^1H\}$ -NMR (125 MHz, $CDCl_3$): δ = 153.6, 152.1, 148.04, 148.3, 141.1, 136.4, 135.6, 132.4, 129.8, 124.6, 123.8, 123.3, 121.4, 121.1, 119.4, 92.2, 55.7, 40.5, 26.6, 23.6, 14.5. HRMS: calc. for $C_{33}H_{34}N_1I_1$: 571.1730 [M] $^+$, found 571.1730. IR (KBr, cm^{-1}): ν = 1611 (m, $C=C_{Flu}$), 1596, 1488 (vs, $C=C_{NPh_2}$). Raman (neat, cm^{-1}): ν = 1614 (s, $C=C_{Flu}$), 1593 (vs, $C=C_{NPh_2}$).

Luminescence measurements. Luminescence measurements in solution were performed in dilute air-saturated solutions contained in quartz cells of 1 cm pathlength (ca. 10^{-6} M, optical density < 0.1) at room temperature (298 K), using an Edinburgh Instruments (FLS920) fluorimeter equipped with a 450 W Xenon lamp and a Peltier-cooled Hamamatsu R928P photomultiplier tube in photon-counting mode. Fully corrected emission spectra were obtained at $\lambda_{ex} = \lambda_{max}^{abs}$ with an optical density at $\lambda_{ex} \leq 0.1$ to minimize internal absorption. Luminescence quantum yields were measured according to literature procedures.^[37,38] UV-vis absorption spectra used for the calculation of the luminescence quantum yields were recorded using a double-beam Jasco V-570 spectrometer. Luminescence lifetimes were measured by time-correlated single photon counting (TCSPC). Excitation was achieved by a hydrogen-filled nanosecond flashlamp (repetition rate 40 kHz) or a pulsed diode laser EPL-440. The instrument response (FWHM ca. 1 ns) was determined by measuring the light scattered by a Ludox suspension. The TCSPC traces were analyzed by standard iterative deconvolution methods implemented in the software of the fluorimeter. Sucrose octaacetate (SOA) was purchased from Acros and purified according to lit.^[23] The SOA glass samples were prepared by typically adding 15 μ L of $5 \cdot 10^{-4}$ M TCBD stock solution in CH_2Cl_2 to 3 g of melted SOA in a test tube. The mixture was homogenized, poured into a quartz fluorescence cell (1 cm \times 1 cm pathlength), and allowed to cool down to room temperature.

Two-photon excited fluorescence measurements. 2PA cross sections (σ_2) of compounds **4-6** were derived from the two-photon excited fluorescence (TPEF) cross sections ($\sigma_2\phi_F$) and the fluorescence emission quantum yield (ϕ_F). TPEF cross sections were measured relative to fluorescein in 0.01 M aqueous NaOH^[39] using the well-established method described by Xu and Webb^[40] and the appropriate solvent-related refractive index corrections.^[41] Reference values between 700 and 715 nm for fluorescein were taken from literature.^[10e] The quadratic dependence of the fluorescence intensity on the excitation power was checked for each sample and all wavelengths. Measurements were conducted using an excitation source delivering fs pulses. A Chameleon Ultra II (Coherent) was used generating 140 fs pulses at 80 MHz repetition rate. The excitation was focused into the cuvette through a microscope objective (10X, NA 0.25). The fluorescence was detected in epifluorescence mode via a dichroic mirror (Chroma 675dcxru) and a barrier filter (Chroma e650sp-2p) by a compact CCD spectrometer module BWTek BTC112E. Total fluorescence intensities were obtained by integrating the corrected emission.

Z-scan Studies on 1-3. Third-order nonlinear optical properties were investigated with an amplified femtosecond laser system using a Clark-MXR CPA-2001 Ti-sapphire regenerative amplifier to pump a Light Conversion TOPAS optical parametric amplifier. Experiments were performed over a wide range of wavelengths using different modes of the OPA output and employing polarizing optics, spatial filtering and colour glass filters to reject unwanted wavelengths. The pulse duration was approximately 150 fs and the repetition rate was 250 Hz. The pulse energy was adjusted to keep the nonlinear phase shifts that were obtained from the samples in the range of roughly 0.3 -1.5 rad, which typically corresponded to light intensities of the order of 100 GW/cm². Solutions of the compounds in dichloromethane of ca. 0.5 w/w% concentration were placed in 1 mm stoppered Starna glass cells. An identical cell was used for measurements of Z-scans on pure solvent. All measurements were calibrated by referencing to signals obtained from a 3 mm thick fused silica plate, and the NLO properties of the solute were determined as described previously.^[42]

Computational Details. Gas phase geometry optimizations of **1-6** were performed by DFT on simplified (**C1-C6**) models (for reasons of computational expediency) where the butyl chains on the fluorene groups have been replaced by methyls. The Gaussian 09 program package (Revision D.01)^[43] was used and the hybrid functional PBE1 which uses 25% exchange and 75% correlation weighting was employed.^[44] This functional has been shown to give very good results in the case of magnetic, vibrational, and electronic properties of molecules, compared to DFT functionals that include extensive parameterization.^[45] In all calculations and for all atoms, all-electron Slater-type orbital basis sets were used (6-31(p)) which includes only polarization function on the heavy atoms. UV-Vis spectra were calculated using time-dependent methods (TD-DFT).^[46]

Acknowledgements

The CNRS and the "Région Bretagne" (ARED) are acknowledged for financial support to N.R, and the Erasmus program and UR1 for financial support to Z.P. A. Bondon (RMN-ILP/UMR 6226) is acknowledged for experimental assistance. M.B. thanks the "Région Bretagne" for a post-doctoral fellowship. K.M. J.O.B. & M.S. acknowledge financing by NCN Maestro grant (DEC-2013/10/A/ST4/00114). M. G. H. thanks the Australian Research Council for support. The support of the Wrocław Centre for Networking and Supercomputing is also acknowledged.

Keywords: Tetracyanobutadiene • Nonlinear Optical Properties • Two-photon Absorption • Luminescence • Alkyne

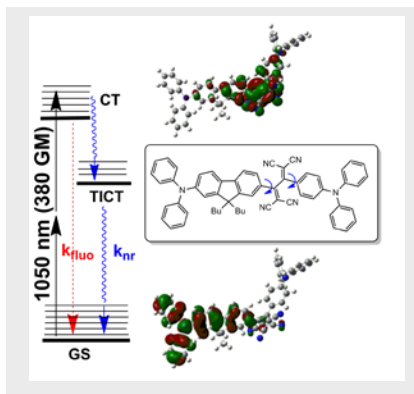
- [1] a) M. Betou, N. Kerisit, E. Meledje, Y. R. Leroux, C. Katan, J.-F. Halet, J.-C. Guillemin, Y. Trolez, *Chem. Eur. J.* **2014**, *20*, 9553-9557; b) T. Shoji, E. Shimomura, M. Maruyama, A. Maruyama, S. Ito, T. Okujima, K. Toyota, N. Morita, *Eur. J. Org. Chem.* **2013**, 7785-7799; c) R. Misra, P. Gautam, S. M. Mobin, *J. Org. Chem.* **2013**, *78*, 12440-12452; d) R. Garcia, M. A. Herranz, M. R. Torres, P.-A. Bouit, J. L. Delgado, J. Calbo, P. M. Viruela, E. Ortí, N. Martín, *J. Org. Chem.* **2012**, *77*, 10707-10717; e) D. Koszelewski, A. Nowak-Król, D. T. Gryko, *Chem. Asian J.* **2012**, *7*, 1887-1894; f) T. Shoji, J. Higashi, S. Ito, T. Okujima, M. Yasunami, N. Morita, *Chem. Eur. J.* **2011**, *17*, 5116-5129; g) X. Tang, W. Liu, J. Wu, C.-S. Lee, J. You, P. Wang, *J. Org. Chem.* **2010**, *75*, 7273-7278; h) S.-I. Kato, M. Kivala, W. B. Schweizer, C. Boudon, J.-P. Gisselbrecht, F. Diederich, *Chem. Eur. J.* **2009**, *15*, 8687-8691; i) T. Shoji, S. Ito, K. Toyota, M. Yasunami, N. Morita, *Chem. Eur. J.* **2008**, *14*, 8398-8408; j) Y. Morioka, N. Yoshizawa, J.-I. Nishida, Y. Yamashita, *Chem. Lett.* **2004**, 33, 1190-1191; k) T. Mochida, S. Yamazaki, *J. Chem. Soc. Dalton Trans.* **2002**, 3559-3564; l) X. Wu, J. Wu, Y. Liu, A. K.-Y. Jen, *J. Am. Chem. Soc.* **1999**, *121*, 472-473.
- [2] C. Cai, I. Liakatas, M.-S. Wong, M. Bösch, C. Bosshard, P. Günter, S. Coniglio, N. Tirelli, U. W. Suter, *Org. Lett.* **1999**, *1*, 1847-1849.
- [3] a) J. C. May, I. Biaggio, F. Bures, F. Diederich, *Appl. Phys. Lett.* **2007**, *90*, 251106/251101-251103; b) J. C. May, J. H. Lim, I. Biaggio, N. P. Moonen, T. Michinobu, F. Diederich, *Opt. Lett.* **2005**, *30*, 3057-3059; c) T. Michinobu, J. C. May, J. H. Lim, C. Boudon, J.-P. Gisselbrecht, P. Seiler, M. Gross, I. Biaggio, F. Diederich, *Chem. Commun.* **2005**, 737-739.
- [4] a) S.-I. Kato, F. Diederich, *Chem. Commun.* **2010**, 46, 1994-2006; b) M. Kivala, F. Diederich, *Acc. Chem. Res.* **2009**, *42*, 235-248.
- [5] B. Esembeon, M. L. Scimeca, T. Michinobu, F. Diederich, I. Biaggio, *Adv. Mater.* **2008**, *20*, 4584-4587.
- [6] M. T. Beels, M. S. Fleischman, I. Biaggio, B. Breiten, M. Jordan, F. Diederich, *Opt. Mater. Express* **2012**, *2*, 294-303.
- [7] a) N. P. Moonen, R. Gist, C. Boudon, J.-P. Gisselbrecht, P. Seiler, T. Kawai, A. Kishioka, M. Gross, M. Irie, F. Diederich, *Org. Biomol. Chem.* **2003**, *1*, 2032-2034; b) G. S. He, L.-S. Tan, Q. Zheng, P. N. Prasad, *Chem. Rev.* **2008**, *108*, 1245-1330.
- [8] F. Z. Henari, *J. Opt. A: Pure Appl. Opt.* **2001**, *3*, 188-190.
- [9] a) M. Pawlicki, H. A. Collins, R. G. Denning, H. L. Anderson, *Angew. Chem. Int. Ed.* **2009**, *48*, 3244-3266; b) H. M. Kim, B. R. Cho, *Chem. Commun.* **2009**, 153-164.
- [10] a) A. Rebane, M. Drobizhev, N. S. Makarov, E. Beuerman, J. E. Haley, D. M. Krein, A. R. Burke, J. L. Flikkema, T. M. Cooper, *J. Phys. Chem. A* **2011**, *115*, 4255-4262; b) F. Terenziani, C. Katan, E. Badaeva, S. Tretiak, M. Blanchard-Desce, *Adv. Mater.* **2008**, *20*, 4541-4678; c) O. Mongin, L. Porrès, M. Charlot, C. Katan, M. Blanchard-Desce, *Chem. Eur. J.* **2007**, *13*, 1481-1498; d) C.-Y. Chen, Y. Tang, Y.-J. Cheng, A. C. Young, J.-W. Ka, A. K.-Y. Jen, *J. Am. Chem. Soc.* **2007**, *129*, 7220-7221; e) C. Katan, S. Tretiak, M. H. V. Werts, A. J. Bain, R. J. Marsh, N. Leonczek, N. Nicolaou, E. Badaeva, O. Mongin, M. Blanchard-Desce, *J. Phys. Chem. B* **2007**, *111*, 9468-9483; f) O. Mongin, T. R. Krishna, M. H. V. Werts, A.-M. Caminade, J.-P. Majoral, M. Blanchard-Desce, *Chem. Commun.* **2006**, 915-917.
- [11] N. I. Nijegorodov, W. S. Downey, *J. Phys. Chem.* **1994**, *98*, 5639-5643.
- [12] C. Rouxel, M. Charlot, O. Mongin, T. R. Krishna, A.-M. Caminade, J.-P. Majoral, M. Blanchard-Desce, *Chem. Eur. J.* **2012**, *18*, 16450-16462.
- [13] a) T. Michinobu, C. Boudon, J.-P. Gisselbrecht, P. Seiler, B. Frank, N. N. P. Moonen, M. Gross, F. Diederich, *Chem. Eur. J.* **2006**, *12*, 1889-1905; b) F. Tancini, F. Monti, K. Howes, A. Belbakra, A. Listorti, W. B. Schweizer, P. Reutenauer, J.-L. Alonso-Gomez, C. Chiorboli, L. M. Umer, J.-P. Gisselbrecht, C. Boudon, N. Armaroli, F. Diederich, *Chem. Eur. J.* **2014**, *20*, 202-216; c) F. Monti, A. Venturini, A. Nenov, F. Tancini, A. D. Finke, F. Diederich, N. Armaroli, *J. Phys. Chem. A* **2015**, *119*, 10677-10683.
- [14] a) X. Yang, Y. Zhao, X. Zhang, R. Li, J. Dang, Y. Li, G. Zhou, Z. Wu, D. Ma, W.-Y. Wong, X. Zhao, A. Ren, L. Wang, X. Hou, *J. Mater. Chem.* **2012**, *22*, 7136-7148; b) C. Cheng, W. Wu, H. Guo, S. Ji, P. Song, K. Han, J. Zhao, X. Zhang, Y. Wu, G. Du, *Eur. J. Inorg. Chem.* **2010**, 4683-4696.

- [15] a) F. Malvolti, C. Rouxel, O. Mongin, P. Hapiot, L. Toupet, M. Blanchard-Desce, F. Paul, *Dalton Trans.* **2011**, 40, 6616-6618; b) F. Paul, *work in progress*.
- [16] K. D. Belfield, M. V. Bondar, *J. Phys. Org. Chem.* **2003**, 16, 194-201.
- [17] G. Grelaud, M. P. Cifuentes, T. Schwich, G. Argouarch, S. Petrie, R. Stranger, F. Paul, M. G. Humphrey, *Eur. J. Inorg. Chem.* **2012**, 65-75.
- [18] A. Weller, *Z. Phys. Chem. N. F.* **1982**, 133, 93-98.
- [19] In this equation, e is the electron charge, ϵ_0 is the dielectric constant in vacuum, ϵ is the relative dielectric constant and a is the distance between the positive and negative charge in the CT state. Based on the computed HOMO and LUMO for each compound, the later was obtained by considering the distance between the most electronegative nitrogen atom and midpoint of the nearby TCBD unit.
- [20] D. Cao, Z. Liu, Y. Deng, G. Li, G. Zhang, *Dyes and Pigments* **2009**, 83, 348-353.
- [21] A. M. Brouwer, *Pure Appl. Chem.* **1980**, 83, 2213-2228.
- [22] a) B. Valeur, *Molecular Fluorescence: Principles and Applications*, Wiley-VCH Verlag GmbH, Weinheim, **2001**; b) W. Rettig, *Angew. Chem.* **1986**, 98, 636-986.
- [23] G. Jones, II, D. Yan, J. Hu, J. Wan, B. Xia, V. I. Vullev, *J. Phys. Chem. B* **2007**, 111, 6921-6929.
- [24] Q. Bellier, N. S. Makarov, P.-A. Bouit, S. Rigaut, K. Kamada, P. Feneyrou, G. Berginc, O. Maury, J. W. Perry, C. Andraud, *Phys. Chem. Chem. Phys.* **2012**, 14, 15299-15307.
- [25] M. G. Kuzyk, *J. Chem. Phys.* **2003**, 119, 8327-8334.
- [26] M. G. Kuzyk, *J. Mater. Chem.* **2009**, 19, 7444-7465.
- [27] Similar 2PA cross-sections were determined from TPEF and Z-scan for **4**, validating the comparison between 2PA values determined by different methods for both sets of compounds.
- [28] J. M. Hales, J. Matchak, S. Barlow, S. Ohira, K. Yesudas, J.-L. Brédas, J. W. Perry, S. R. Marder, *Science* **2010**, 327, 1485-1488.
- [29] T. Jadhav, R. Maragani, R. Misra, V. Sreeramulu, D. N. Rao, S. M. Mobin, *Dalton Trans.* **2013**, 42, 4340-4342.
- [30] G. Grelaud, M. P. Cifuentes, F. Paul, M. G. Humphrey, *J. Organomet. Chem.* **2014**, 751, 181-200 (150th Anniversary Special Issue).
- [31] J. P. Merrick, D. Moran, L. Radom, *J. Phys. Chem. A* **2007**, 111, 11683-11700.
- [32] C. Adamo, D. Jacquemin, *Chem. Soc. Rev.* **2013**, 42, 845-856 and refs therein.
- [33] D. F. Shriver, M. A. Drezdson, *The Manipulation of Air-Sensitive Compounds*, Wiley and sons, New-York, **1986**.
- [34] F. Xu, L. Peng, A. Orita, J. Otera, *Org. Lett.* **2012**, 14, 3970-3973.
- [35] a) D. Li, H. Li, M. Liu, J. Chen, J. Ding, X. Huang, H. Wu, *Macromol. Chem. Phys.* **2014**, 215, 82-89; b) F. Li, Z. Chen, W. Wei, H. Cao, Q. Gong, F. Teng, L. Qian, Y. Wang, *J. Phys. D: Appl. Phys.* **2004**, 37, 1613-1616.
- [36] N. G. Connelly, W. E. Geiger, *Chem. Rev.* **1996**, 96, 877-910.
- [37] N. Demas, G. A. Crosby, *J. Phys. Chem.* **1971**, 75, 991-1024.
- [38] D. F. Eaton, *Pure Appl. Chem.* **1988**, 60, 1107-1114.
- [39] M. A. Albota, C. Xu, W. W. Webb, *Appl. Opt.* **1998**, 37, 7352-7356.
- [40] C. Xu, W. W. Webb, *J. Opt. Soc. Am. B* **1996**, 13, 481-491.
- [41] M. H. V. Werts, N. Nerambourg, D. Pélégry, Y. Le Grand, M. Blanchard-Desce, *Photochem. Photobiol. Sci.* **2005**, 4, 531-538.
- [42] a) M. Samoc, A. Samoc, G. T. Dalton, M. P. Cifuentes, M. G. Humphrey, P. A. Fleitz, in *Multiphoton Processes in Organics and Their Application* (Eds.: I. Rau, F. Kajzar), Old City Publishing, Philadelphia, **2011**, pp. 341-355; b) B. Babgi, L. Rigamonti, M. P. Cifuentes, T. C. Corkery, M. D. Randles, T. Schwich, S. Petrie, R. Stranger, A. Teshome, I. Asselberghs, K. Clays, M. Samoc, M. G. Humphrey, *J. Am. Chem. Soc.* **2009**, 131, 10293-10307.
- [43] M. J. Frisch, G. W. Trucks, H. B. Schlegel, G. E. Scuseria, M. A. Robb, J. R. Cheeseman, G. Scalmani, V. Barone, B. Mennucci, G. A. Petersson, H. Nakatsuji, M. Caricato, X. Li, H. P. Hratchian, A. F. Izmaylov, J. Bloino, G. Zheng, J. L. Sonnenberg, M. Hada, M. Ehara, K. Toyota, R. Fukuda, J. Hasegawa, M. Ishida, T. Nakajima, Y. Honda, O. Kitao, H. Nakai, T. Vreven, J. A. Montgomery (Jr.), J. E. Peralta, F. Ogliaro, M. Bearpark, J. J. Heyd, E. Brothers, K. N. Kudin, V. N. Staroverov, R. Kobayashi, J. Normand, K. Raghavachari, A. Rendell, J. C. Burant, S. S. Iyengar, J. Tomasi, M. Cossi, N. Rega, N. J. Millam, M. Klene, J. E. Knox, J. B. Cross, V. Bakken, C. Adamo, J. Jaramillo, R. Gomperts, R. E. Stratmann, O. Yazyev, A. J. Austin, R. Cammi, C. Pomelli, J. W. Ochterski, R. L. Martin, K. Morokuma, V. G. Zakrzewski, G. A. Voth, P. Salvador, J. J. Dannenberg, S. Dapprich, A. D. Daniels, Ö. Farkas, J. B. Foresman, J. V. Ortiz, J. Cioslowski, D. J. Fox, Gaussian, Inc., Wallingford CT, **2009**.
- [44] J. P. Perdew, K. Burke, M. Ernzerhof, *Phys. Rev. Lett.* **1996**, 77, 3865-3868.
- [45] G. A. A. Saracino, R. Improta, V. Barone, *Chem. Phys. Lett.* **2003**, 373, 411-415.
- [46] E. Runge, E. K. U. Gross, *Phys. Rev. Lett.* **1984**, 52, 997-1000.

Entry for the Table of Contents

FULL PAPER

Selected optical properties of four new tetracyanobutadiene derivatives incorporating fluorenyl and diphenylamino moieties have been studied. While non-luminescent in solution at ambient temperatures, these electroactive derivatives become luminescent in more rigid media. They are also two-photon absorbers in the near-IR range (800-1050 nm).



Ziemowit Pokladek, Nicolas Ripoche, Marie Betou, Yann Trolez, Olivier Mongin, Joanna Olesiak-Banska, Katarzyna Matczyszyn, Marek Samoc, Mark G. Humphrey, Mireille Blanchard-Desce and Frédéric Paul*

Page No. – Page No.

Linear Optical and Third-Order Nonlinear Optical Properties of Some Fluorenyl- and Triarylamine-Containing Tetracyanobutadiene Derivatives